

# Synthesis and phase behaviour of liquid crystalline polyesters derived from *p,p'*-bibenzoic acid and *meso* and *R*-3-methylhexanediol

Aránzazu del Campo, Ernesto Pérez, Rosario Benavente\*, Antonio Bello and José M. Pereña

*Instituto de Ciencia y Tecnología de Polímeros, CSIC, Juan de la Cierva 3, 28006 Madrid, Spain*

(Received 18 November 1997)

The synthesis and thermal properties of two new liquid crystalline polyesters derived from bibenzoic acid and (R,S)- or (R)-3-methyl-1,6-hexanediol are reported. The phase behaviour was investigated by means of differential scanning calorimetry, X-ray diffraction and polarizing microscopy. The effect of the asymmetry introduced by the branched methyl group and that of the stereoisomerism on the type and stability of the mesophases formed are analysed. Both polymers exhibited smectic mesophases of different types depending on thermal history. The presence of an optically active pure diol along the chain gives rise to a more regular structure in comparison with the polymer synthesized from the racemic mixture. © 1998 Published by Elsevier Science Ltd. All rights reserved.

(Keywords: liquid crystalline polymers; phase behaviour; thermotropic polybibenzoates)

## INTRODUCTION

Several works have been published concerning the thermotropic liquid crystal character of polyesters derived from bibenzoic acid and different methylenic<sup>1–3</sup> or oxy-methylenic<sup>4–9</sup> spacers, in an effort to study the influence of the nature of the spacer on the properties related with the type and/or stability of the mesophase formed. The biphenyl group in these polymers is able to generate smectic mesophases with an isotropization temperature which generally decreases with the length of the spacer. Moreover, the spacer plays a very important role in determining the phase behaviour of these systems, as well as the type of mesophase formed. The polymer molecule in the liquid crystalline phase must adopt a conformation and packing compatible with the symmetry properties of that mesophase. Changes in the stiffness of the spacer, which is related to the number of conformations permitted to the system, is primarily determined by the bulkiness of the side groups and may influence the molecular packing in the mesophase and its properties.

From the structural point of view, the type of smectic mesophase depends on the chemical nature or geometry of the spacer. For linear spacers with an even number of methylenes the most common structure is the  $S_A$ , but this is transformed for an odd number of methylenic groups in an inclined mesophase with biaxial symmetry<sup>10</sup>,  $S_{C2}$ . Moreover,  $S_C$  mesophases have been reported for spacers with oxygen groups like triethyleneglycol<sup>11</sup> and also with methyl substituents in the hydrocarbonated spacers<sup>12,13</sup>. Materials which form chiral smectic C ( $S_C^*$ ) phases are highly sought after because  $S_C^*$  structures are ferroelectric and

spontaneously polarize if the helix is unwound. The potential applications of these mesophases take advantage of their ability to freeze an anisotropic alignment below the glass transition.

The interest in this kind of material prompted us to synthesize an asymmetric diol, like the (R-) and meso forms of 3-methyl hexanediol. The corresponding polybibenzoates have been prepared in order to analyse the effect of the asymmetry introduced by the lateral group on the phase behaviour. The influence of the optical activity is also studied.

## EXPERIMENTAL

Both meso and (R)-3-methyl-1,6-hexanediol were prepared by reduction of the corresponding 3-methyldiethyl adipate with lithium aluminium hydride dissolved in diethylether<sup>14</sup>. The diesters were synthesized from the corresponding 3-methyladipic acid by refluxing in an excess of ethanol with a trace of sulfuric acid, according to the esterification procedure of Fischer–Speier<sup>15</sup>. The starting material for obtaining the optically active diol was the (R)-3-methyladipic acid,  $[\alpha]^{21} = +7.2$  (Aldrich). The diesters and diols were purified by reduced pressure distillation. Their boiling points are 141°C (diesters) and 163°C (diols) at 13 torr.

The polymers were synthesized by melt transesterification of diethyl *p,p'*-bibenzoate and the corresponding diol using isopropyl titanate as a catalyst. The polyesters were purified by dissolving in chloroform and precipitating in excess methanol. The polymers obtained were poly((R)-3-methylhexamethylene *p,p'*-bibenzoate) (R-P6), and poly((R,S)-3-methylhexamethylene *p,p'*-bibenzoate),

\* To whom correspondence should be addressed

(R,S-P6). The structural formula of the polymers (and the carbon designations) is the following:

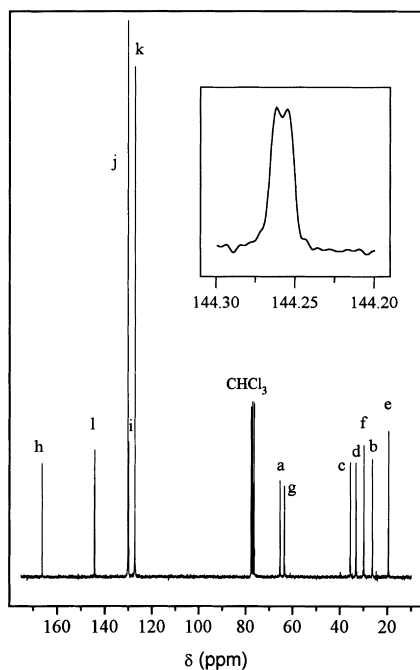
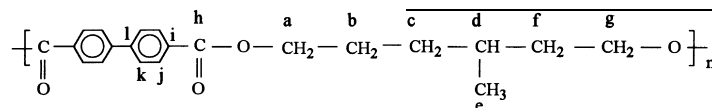


**Figure 1**  $^{13}\text{C}$ -n.m.r. spectrum at 125 MHz of R-P6 in deuterated chloroform at 45°C showing the assignment to the different carbons. The amplified inset corresponds to quaternary carbons l

**Table 1** Values of chemical shifts corresponding to  $^{13}\text{C}$ -n.m.r. spectrum at 125 MHz of poly((R,S)-3-methylhexamethylene *p,p'*-bibenzoate)

Carbon	$\delta_{\text{calc}}$ (ppm)	$\delta_{\text{exp}}$ (ppm)
a	65.3	65.23
b	26.2	26.21
c	35.5	35.56
d	33.2	33.14
e	19.5	19.43
f	29.8	29.85
g	63.3	63.41
h	166.8	166.19
i	129.6	130.00
j	130.2	130.06
k	127.4	127.12
l	145.9	144.26

$^{13}\text{C}$ -n.m.r. measurements were carried out in a Varian Unity 500 spectrometer in deuterated chloroform at 45°C. The  $^{13}\text{C}$ -n.m.r. spectrum of R-P6 is shown in *Figure 1*, with the assignment of the different carbons. The corresponding experimental and calculated chemical shifts are presented in *Table 1*. If the Fourier transformation in the  $^{13}\text{C}$ -n.m.r. spectrum is performed with 512 K points, a splitting of the resonances corresponding to carbons h, l and j is observed. The splitting for the quaternary carbon l is shown in the amplified inset of *Figure 1*. It is of the order of 0.90 Hz, while it takes the value of 0.70 Hz for the carbonyl and 1.0 Hz for carbon j. These splittings are simply a consequence of the asymmetry of the spacer, leading to small chemical shift differences in the two benzoate groups of each side, and thus, to two signals of equal area.

Along the polymer backbone, head-to-head, head-to-tail and tail-to-tail arrangements are expected to be randomly

distributed, due to the fact that both hydroxyl groups of the diol have presumably similar reactivities because of their

distances to the asymmetric carbon. Moreover, in the case of R,S-P6, as we are dealing with a racemic mixture of diols, the two stereo-isomers are also expected to be randomly arranged along the polymer chain.

The rotatory power of the chiral precursors and polymers was determined in chloroform solution at 21°C in a Perkin-Elmer 241MC spectrometer. The values obtained were:  $[\alpha]_D^{21} = +3.9$  for (R)-3-methyldiethyl adipate,  $+3.2$  for (R)-3-methyl-1,6-hexanediol and  $+29.2$  for R-P6.

Size exclusion chromatography measurements were performed at 28°C in a Waters 150C equipment, in chloroform. A set of two mixed beds of 10  $\mu\text{m}$  of PL Gel columns were used. The operating conditions were as follows: flow rate 1.0 ml/min, sample concentration 5 mg/ml, and injection volume 200  $\mu\text{l}$ . Twelve samples of monodisperse polystyrene (with molecular weights ranging from 1800 to 2 300 000) were used as standards. A DRI detector and a differential viscometer Viscotek 110, working at 28°C, were coupled at the end of the columns. The molecular weight results are shown in *Table 2*.

The intrinsic viscosity of the polymers was measured at 25°C in chloroform by using an Ubbelohde viscometer, previously calibrated, in conjunction with a Lauda Viscotimer S/2 flow-time measuring unit. Precision in efflux times was  $\pm 0.025$  s. The temperature was controlled by using an electronic Unicontrol R325 Lauda unit. Temperature precision was  $\pm 0.02^\circ\text{C}$ . The values of intrinsic viscosity  $[\eta]$  and constant ( $k$ ) were calculated by using the Huggins<sup>16</sup>, Kraemer<sup>17</sup>, Heller<sup>18</sup> and Schulz-Blaschke<sup>19</sup> equations (*Table 2*).

Differential scanning calorimetric measurements were carried out with a Perkin Elmer DSC7 calorimeter connected to a cooling system. Samples of 8–10 mg were used. Polarizing microscopy did not give any satisfactory results due to the high molecular weight of the polymers, even when birefringent textures were found.

Wide-angle X-ray diffraction photographs were taken with a flat plate camera. The distance from sample to film was determined by using aluminium foil as standard. Nickel filtered  $\text{CuK}\alpha$  radiation was used. Polymer films for X-ray measurements were prepared in a Collin press fitted with smooth-polished plates. The polymer samples were hot pressed above the melting temperature and then cooled at constant pressure either by quenching the polymer between two water-cooled plates or by slow cooling without pressure. Oriented films were obtained by uniaxial stretching.

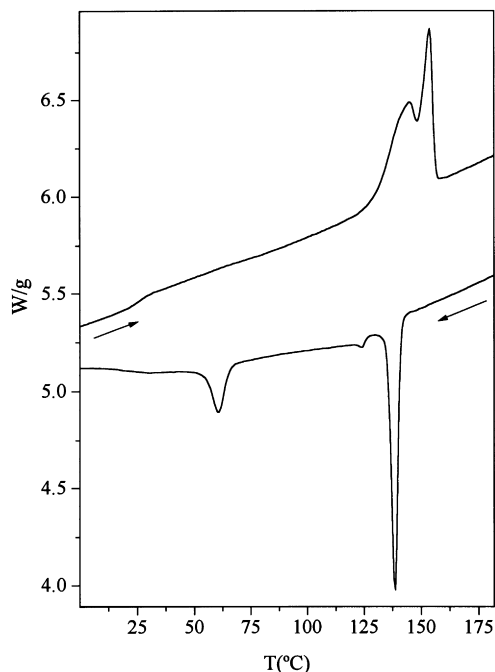
## RESULTS

### *Poly((R,S)-3-methylhexamethylene *p,p'*-bibenzoate), R,S-P6*

The d.s.c. curves for R,S-P6 are shown in *Figure 2*. Three exotherms at 139, 124 and 61°C are obtained on cooling from the isotropic melt. In the subsequent heating cycle two endotherms at 145 and 154°C appear. The transition at 145°C shows a wide and asymmetric shape, which suggests the participation of two partially overlapped peaks. The general shape of these curves is similar to those published

**Table 2** Values of molecular weights, and intrinsic viscosity ( $[\eta]$ ) and constants ( $k$ ) corresponding to the Huggins, Kraemer, Heller and Schulz-Blaschke equations

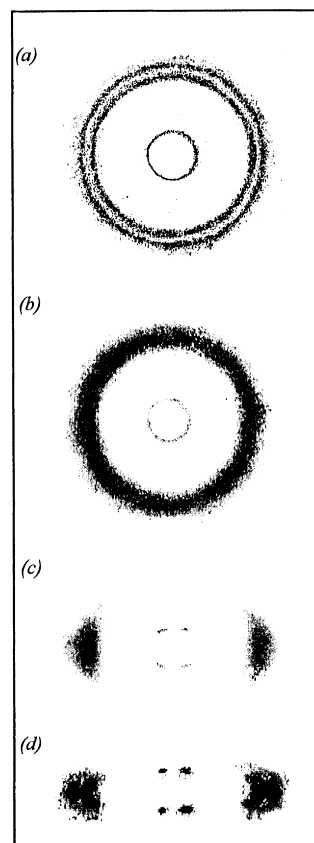
Sample	$10^{-4} M_n$	$M_w/M_n$	$[\eta]$ (dl/g)				
			Huggins <sup>16</sup>	Kraemer <sup>17</sup>	Heller <sup>18</sup>	Heller <sup>18</sup>	Schulz-Blaschke <sup>19</sup>
R,S-P6	1.803	1.936	0.533 $k_H = 0.43$	0.535 $k_K = 0.11$	0.539 $k_H = 0.33$	0.536 $k_K = 0.12$	0.539 $k_{SB} = 0.35$
R-P6	1.718	2.968	0.649 $k_H = 0.49$	0.653 $k_K = 0.11$	0.659 $k_H = 0.32$	0.654 $k_K = 0.12$	0.659 $k_{SB} = 0.32$

**Figure 2** D.s.c. curves of R,S-P6 corresponding to the cooling from the melt (lower) and the subsequent melting (upper). Scanning rate was 20°C/min

for poly(2-methyltetramethylene *p,p'*-bibenzoate)<sup>20,21</sup>. Considering these results, the magnitude of the enthalpy change and the small undercooling, the first transition in the cooling experiment (139°C) is attributed to the formation of a smectic mesophase which transforms subsequently in other phases of more symmetry. The  $T_g$  of the polymer can be also observed at 24°C.

In order to clarify the nature of the transitions detected by d.s.c. measurements, several X-Ray diffractograms were taken at different conditions. *Figure 3a* shows the diffraction pattern recorded at room temperature for a sample slowly cooled from the melt. Under these conditions of cooling, the most ordered phase, which appears at 61°C in the d.s.c. curves (*Figure 2*), must be formed. The diffractogram presents two sharp outer reflections and one sharp inner ring. The sharp inner ring corresponds to 17.2 Å and is attributed to the spacing between layers in a smectic mesophase. The outer diffractions at 4.4 and 5.1 Å indicate the presence of order in the lateral arrangement of segments in the layer. Moreover, these spacings fulfil the relation  $d/\sqrt{3}$  and  $d/2$ . This pattern is typical of smectic mesophases with hexagonal packing parallel to the long axes of the molecules.

*Figure 3b* shows the diffraction pattern of an unoriented sample obtained by quenching from the isotropic melt to ambient temperature. It consists of a sharp inner reflection attributed to the smectic layer spacing and a diffuse outer

**Figure 3** WAXD photographs of R,S-P6 taken at room temperature: (a) unoriented sample slowly cooled from the melt, (b) unoriented sample quenched from the melt, (c) quenched specimen stretched at room temperature, (d) the same specimen as in (c) stretched at 80°C. Draw direction vertical

halo corresponding to a disordered lateral arrangement of the molecules in the mesophase. This kind of pattern is typical of  $S_A$  or  $S_C$  mesophases. Under these quenching conditions the formation of the hexagonal structure is inhibited (see below) and this pattern corresponds to one of the phases which appears between the isotropic melt and the transition at 61°C.

The smectic layer spacing deduced from the inner ring takes the value of 17.2 Å, while the fully extended length of the repeating unit of the poly(hexamethylene *p,p'*-bibenzoate) is 20.0 Å<sup>22</sup>. Hence, either the repeating units are tilted with respect to the normal layer, or the hydrocarbon portion of the repeating unit does not have its fully extended all-*trans* conformation.

If the quenched sample is uniaxially oriented at ambient temperature, the pattern of *Figure 3c* is obtained, where two diffuse outer arcs appear with the maximum of intensity on the equatorial plane and four symmetric spots at both sides of the meridional plane. This pattern is characteristic of a  $S_C$  mesophase, where the repeating units are tilted in relation to

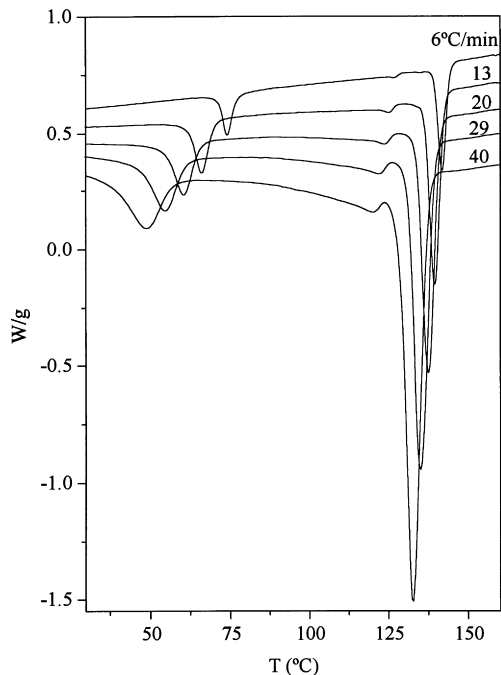


**Figure 4** D.s.c. cooling curves from the melt corresponding to R,S-P6 at the indicated cooling rates

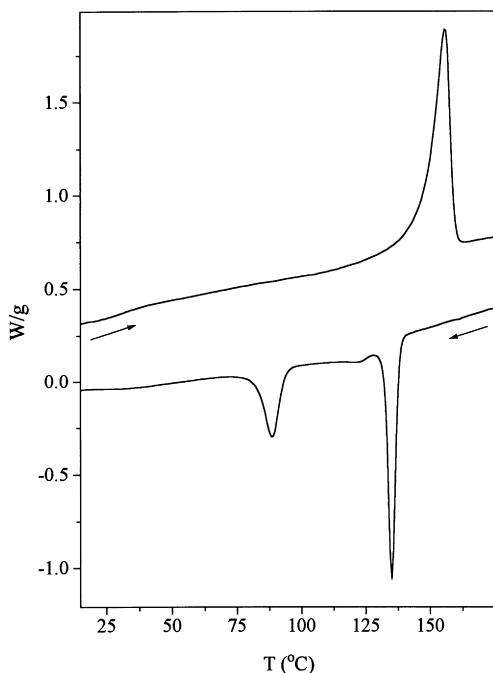


**Figure 5** D.s.c. curves of R-P6 corresponding to the cooling from the melt (lower) and the subsequent melting (upper). Scanning rate was 20°C/min

the smectic layers and there is no lateral order of the molecules within the layer. The tilt angle can be determined from the splitting angle of the inner reflections and is found to be 33°.

Unfortunately, the slowly cooled specimen of *Figure 3a* cannot be stretched to substantial draw ratio since it breaks immediately. Therefore, we decided to anneal the quenched fibre at a temperature sufficiently above the glass transition. If this fibre is heated at 80°C and uniaxially stretched at a slow rate, the diffraction pattern presented in *Figure 3d* is obtained. The comparison with *Figure 3c* shows that the

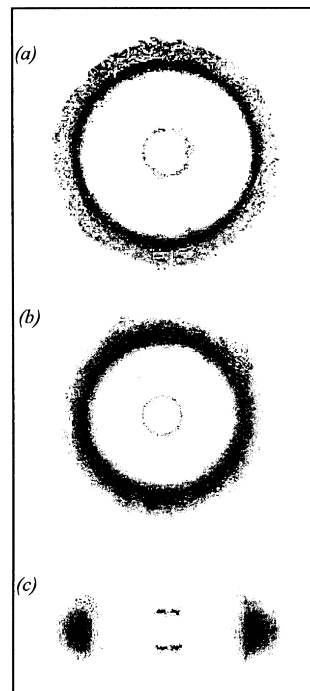


**Figure 6** WAXD photographs of R-P6: (a) unoriented sample slowly cooled from the melt, (b) unoriented sample quenched from the melt, (c) specimen stretched at 80°C. Draw direction vertical

four inner spots keep the same features in both pictures, indicating that both mesomorphic forms possess the long molecular axes tilted with respect to the layer surfaces. There is, however, a remarkable difference, since the diffuse outer diffraction suffers a drastic change. Thus, in *Figure 3c* the diffuse component on the equator indicates a packing of molecules with random lateral disposition. On the contrary, three well-defined spots are observed, two of them appearing at  $2\theta = 19.4^\circ$  and the other at  $22.7^\circ$ , showing an increase in the lateral order. These features indicate the presence of a tilted smectic mesophase with hexagonal packing. The diffraction at  $2\theta = 19.4^\circ$  is split above and below the equator and the one at  $22.7^\circ$  remains on the equator. It seems that the more ordered mesophase that is formed by annealing or slow cooling to room temperature veered the tilting direction towards an apex or a side of the hexagon<sup>23</sup>.

The effect of cooling rate on the transitions obtained by d.s.c. is shown in *Figure 4*. It can be observed that the onset of the two higher temperature transitions are not very dependent on the cooling rate. It is expected, therefore, that these transitions will require extremely fast quenching conditions to avoid their formation. On the contrary, the low temperature transition depends very much on the cooling rate and, considering that  $T_g$  appears at 24°C, it can be deduced that for cooling rates somewhat higher than 40°C/min this transition will be prevented (the cooling system of our calorimeter does not allow us to use higher cooling rates in the region of interest).

The conclusion from these d.s.c. and X-ray experiments is the following: starting from the melt, the first d.s.c. exotherm of R,S-P6 should correspond, probably, to a smectic  $S_A$  mesophase, judging from the characteristics of the peak. This mesophase is immediately transformed into a  $S_C$  phase, which can be easily quenched and identified. This  $S_C$  mesophase is transformed into a hexagonal one, either by slow cooling or by annealing the quenched sample at 80°C.

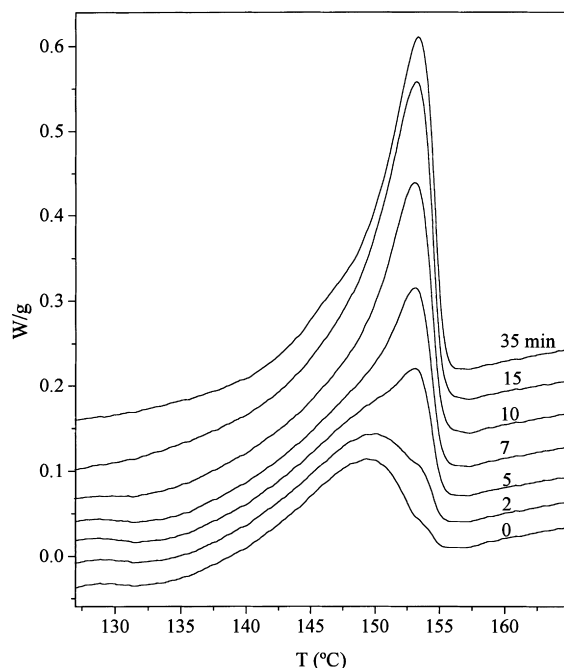


**Figure 7** D.s.c. melting endotherms for R-P6 after isothermal crystallization at 115°C for the indicated times, starting from the isotropic melt. Scanning rate was 5°C/min

#### *Poly((R)-3-methylhexamethylene p,p'-bibenzoate), R-P6*

The d.s.c. cycles for R-P6 are presented in *Figure 5*. The cooling curve shows three exotherms at 135, 122 and 89°C with a shape similar to that aforementioned for R,S-P6. The  $T_g$  of the polymer appears at 32°C. The subsequent heating cycle presents only one melting peak at 157°C. This result suggests a monotropic behaviour for R-P6 similar to that found for other polybibenzoates<sup>24,25</sup>. An X-ray study analogous to that described for R,S-P6 was made for R-P6. Mesophases of  $S_C$  and hexagonal type were found i.e. the phase behaviour is similar to that for R,S-P6. The diffraction patterns are shown in *Figure 6*.

To confirm whether the single endotherm corresponds to a real monotropic behaviour or if it is comprised of two peaks in a narrow interval of temperatures, several isothermal d.s.c. experiments were performed. The heating curves for a sample which was 'crystallized' at 115°C for different time periods, starting from the isotropic melt, are shown in *Figure 7*. At this temperature, the formation of the hexagonal phase is obtained at the time scale of the calorimeter, while the two other mesophases have been formed very rapidly, before temperature equilibration in the calorimeter. The lower curve in *Figure 7*, after zero 'crystallization' time at 115°C, corresponds to the isotropization of the  $S_C$  mesophase, centred at 150°C. The other curves show the appearance of a second melting endotherm at 153°C, the intensity of which increases with the crystallization time. The intensity of the lower temperature peak diminishes simultaneously and disappears almost completely after 15 min of crystallization, i.e. when the  $S_C$  mesophase has been totally transformed into the more ordered hexagonal one. The second peak corresponds to the isotropization of this more ordered phase. Therefore, a monotropic behaviour is observed due to the fact that the isotropization temperature of the  $S_C$  mesophase is lower than that for the pseudohexagonal one.

The very small enthalpy of the transformation of the possible  $S_A$  mesophase into the  $S_C$  one prevents us knowing

whether the  $S_C$  mesophase melts directly into the isotropic melt or if it is transformed first into the  $S_A$  mesophase.

## DISCUSSION

The presence of a methyl group and the random character of the reaction between diethyl *p,p'*-bibenzoate and the asymmetric diol have a significant effect on the mesophase behaviour. Comparing the values of the isotropization temperatures published for poly(hexamethylene *p,p'*-bibenzoate) (> 200°C)<sup>26</sup> and those found for the branched polyesters studied in this paper ( $\approx$  160°C), a significant decrease is found owing to the alteration of the symmetry in the chain caused by the presence of the methyl group, which reduces the lateral packing interaction of chains.

A second effect can be seen on the type of mesophase. Poly(hexamethylene *p,p'*-bibenzoate) presents a  $S_A$  mesophase, which is transformed into a crystal structure on cooling. The branched methyl group tends to transform the  $S_A$  to the  $S_C$  mesophase, according to the results obtained by X-ray diffraction, and in analogy to those published for poly(2-methyltetramethylene *p,p'*-bibenzoate)<sup>12</sup>. These effects have been explained as due to the steric hindrance of the branched methyl groups. Their accommodation into the mesophase structure is achieved by tilted association of polymer chains, and no conformational change or random packing as in nematic structures is needed.

R,S-P6 shows enantiotropic behaviour, while R-P6 is monotropic. Moreover, R-P6 presents a  $T_g$  (32°C) higher than R,S-P6 (24°C). It is well known, however, that the phase behaviour is very much dependent on molecular weight. In fact,  $M_w$  and intrinsic viscosity are significantly higher for R-P6 (although  $M_n$  is slightly smaller) and this might be the reason for the differences in the phase behaviour.

The d.s.c. analysis of R,S-P6 shows the formation of three different phases on cooling from the isotropic melt. According to the d.s.c. and X-ray results, we suggest a phase sequence for R,S-P6 on cooling as follows:  $S_A$ ,  $S_C$ , hexagonal tilted smectic ( $S_F$  or  $S_D$ ). A similar phase behaviour has been found for R-P6, with the only difference being that this polymer presents a monotropic behaviour on melting.

## ACKNOWLEDGEMENTS

The financial support of the Comisión Interministerial de Ciencia y Tecnología (project DGICYT PB94-1529) and of Fundación Ramón Areces is gratefully acknowledged. Prof. I. Hernández-Fuentes is thanked for her contribution to the viscosity analysis and M. Fernández is also thanked for performing the g.p.c. measurements.

## REFERENCES

1. Watanabe, J., Hayashi, M., Morita, A. and Niiori, T., *Mol. Cryst. Liq. Cryst.*, 1994, **254**, 221.
2. Watanabe, J. and Hayashi, M., *Macromolecules*, 1988, **21**, 278.
3. Bello, A., Riande, E., Pérez, E., Marugán, M. M. and Pereña, J. M., *Macromolecules*, 1993, **26**, 1072.
4. Benavente, R., Pereña, J. M., Bello, A. and Pérez, E., *Polymer Bull.*, 1995, **34**, 635.
5. Bello, A., Riande, E., Pérez, E. and Benavente, R., *Macromol. Symp.*, 1994, **84**, 297.
6. Benavente, R., Pereña, J. M., Pérez, E., Bello, A. and Lorenzo, V., *Polymer*, 1994, **35**, 3686.

7. Pérez, E., Marugán, M. M., Bello, A. and Pereña, J. M., *Polymer Bull.*, 1994, **32**, 319.
8. Benavente, R., Pereña, J. M., Pérez, E. and Bello, A., *Polymer*, 1993, **34**, 2344.
9. Pérez, E., Marugán, M. M. and Vanderhart, D. L., *Macromolecules*, 1993, **26**, 5852.
10. Watanabe, J. and Kinoshita, S., *J. Phys. II France*, 1992, **2**, 1237.
11. Pérez, E., Riande, E., Bello, A., Benavente, R. and Pereña, J. M., *Macromolecules*, 1992, **25**, 605.
12. Watanabe, J., Hayashi, M., Kinoshita, S. and Niori, T., *Polymer J.*, 1992, **24**, 597.
13. Loman, A. J. B., Does, L. V. D., Bantjes, A. and Vulic, I., *J. Polym. Sci. Polym. Chem.*, 1995, **33**, 493.
14. Vogel, A. I., *Textbook of Practical Organic Chemistry*, 4th edn. Longman Scientific and Technical, New York, 1987.
15. Haslam, E., *Tetrahedron*, 1980, **36**, 2409.
16. Huggins, M. L., *J. Am. Chem. Soc.*, 1942, **64**, 2716.
17. Kraemer, E. O., *Ind. Eng. Chem.*, 1938, **30**, 1200.
18. Heller, W., *J. Colloid. Sci.*, 1954, **9**, 547.
19. Schulz, G. V. and Blaschke, J. F., *J. Pract. Chem.*, 1941, **158**, 130.
20. Loman, A. J. B., Van der Does, L., Bantjes, A. and Vulic, I., *J. Polym. Sci., Polym. Chem.*, 1995, **33**, 493.
21. Watanabe, J., Komura, H. and Niori, T., *Liq. Cryst.*, 1993, **13**, 455.
22. Li, X. and Brisse, F., *Macromolecules*, 1994, **27**, 7725.
23. Cheng, S. Z. D., Yoon, Y., Zhang, A., Savitski, E. P. and Park, J.-Y., *Macromol. Rapid Commun.*, 1995, **16**, 533.
24. Pérez, E., Zhen, Z., Bello, A., Benavente, R. and Pereña, J. M., *Polymer*, 1994, **84**, 297.
25. Pérez, E., Bello, A., Marugán, M. M. and Pereña, J. M., *Polym. Commun.*, 1990, **23**, 905.
26. Tokita, M., Takahashi, T., Hayashi, M., Inomata, K. and Watanabe, J., *Macromolecules*, 1996, **29**, 1345.